

Effect of quantum dot size and size distribution on the intersublevel transitions and absorption coefficients of III-V semiconductor quantum dot

Sanjib Kabi and A. G. Unil Perera

Citation: *Journal of Applied Physics* **117**, 124303 (2015); doi: 10.1063/1.4916372

View online: <http://dx.doi.org/10.1063/1.4916372>

View Table of Contents: <http://scitation.aip.org/content/aip/journal/jap/117/12?ver=pdfcov>

Published by the *AIP Publishing*

Articles you may be interested in

[Effects of magnetic field and the built-in internal fields on the absorption coefficients in a strained wurtzite GaN/AlGaIn quantum dot](#)

AIP Conf. Proc. **1512**, 1012 (2013); 10.1063/1.4791386

[A simple analysis of interband absorption in quantum well structure of III-V ternary and quaternary semiconductors](#)

J. Appl. Phys. **111**, 103104 (2012); 10.1063/1.4718414

[Terahertz electro-absorption effect enabling femtosecond all-optical switching in semiconductor quantum dots](#)

Appl. Phys. Lett. **97**, 231108 (2010); 10.1063/1.3515909

[Effects of absorption coefficients and intermediate-band filling in InAs/GaAs quantum dot solar cells](#)

Appl. Phys. Lett. **97**, 193106 (2010); 10.1063/1.3516468

[Effects of a Gaussian size distribution on the absorption spectra of III-V semiconductor quantum dots](#)

J. Appl. Phys. **102**, 084305 (2007); 10.1063/1.2798986

Frustrated by old technology? Is your AFM dead and can't be repaired? Sick of bad customer support?



It is time to upgrade your AFM
Minimum \$20,000 trade-in discount for purchases before August 31st

Asylum Research is today's technology leader in AFM

dropmyoldAFM@oxinst.com



The Business of Science®

Effect of quantum dot size and size distribution on the intersublevel transitions and absorption coefficients of III-V semiconductor quantum dot

Sanjib Kabi and A. G. Unil Perera^{a)}

Department of Physics and Astronomy, Georgia State University, Atlanta, Georgia 30303, USA

(Received 3 September 2014; accepted 14 March 2015; published online 25 March 2015)

The intersublevel absorption peak energy and absorption coefficient of non-uniform quantum dot (QD) ensembles are calculated analytically. The effect of size variations and size distribution of QDs on their energy states is analyzed. The dots are considered as a quantum box with finite potential at the barriers and the size distribution described by a Gaussian function. The influence of the aspect ratio (base to height ratio) of the QDs on the optical transitions is studied. Our model predicts the dot size (height and base) accurately to determine the absorption peaks and corresponding absorption coefficient. We also compute the absorption coefficient of the QD with different size distributions to verify the results calculated using this model with the reported experimental and other theoretical results. © 2015 AIP Publishing LLC.

[<http://dx.doi.org/10.1063/1.4916372>]

I. INTRODUCTION

III–V compound semiconductor quantum dots (QDs) are being increasingly used in the fabrication of optoelectronic devices,¹ such as lasers² and detectors.³ These devices respond to normal incidence, have the potential to operate at high temperatures and have low threshold energy.⁴ Although the detectors using HgCdTe (Refs. 5 and 6) or type II strained layer super lattices (SLS)^{7,8} with materials, such as InAsSb–InSb or InAs–InGaSb, have mature and reliable technologies for long-wavelength detectors, there are still problems in epitaxial growth of HgCdTe based materials due to the presence of large interface instabilities and defect densities as observed from device performance.⁹

Quantum dots are being considered as a method of advancing intersubband detectors.^{10,11} Advances in material growth technologies allowed the successful growth of self-organized QDs.^{12–14} The optical transitions in these devices involve subband to subband or subband to continuum absorption. It is, therefore, of immense interest to examine the possibility of using these quantum dots for intersubband detectors. Self-assembled QDs are particularly attractive candidates for IR detection due to their intrinsic sensitivity to normal incident IR radiation owing to the three-dimensional (3D) confinement of carriers. In addition, quantum dot infrared photodetectors (QDIPs) are expected to have lower dark current.¹⁵ However, for these devices to outperform the existing technologies, the QD structures must have a high density and a uniform size distribution.

When IR photons with energies greater than or equal to the intersubband energy spacing of the QD, interact with the quantum dots, the photons may be absorbed by exciting electrons from the ground state to an excited state or to the

continuum of states above the dots. Besides doping concentration, quantum-dot size and shape also affect the absorption coefficient.

Reports on the calculation of the absorption coefficient and the effect of QD size with infinite barrier quantum boxes¹⁶ or spherical approximation¹⁷ and finite barrier quantum boxes^{18,19} for interband transitions are reported in the literature. However, a realistic approach for intersubband transitions considering the dot size distribution with a finite barrier approximation is not yet intensively studied. The development of a theoretical model for intersubband absorption in an ensemble of III-V quantum dots will advance the understanding of absorption process for the design of efficient QDIPs. Here, we present an analytical model to calculate the absorption peak energy and corresponding absorption coefficient for intersubband transitions for different sets of QD ensembles with different size distributions described by a Gaussian distribution. The QDs are approximated as a 3D box with finite potential at the barriers. This simple model leads us to accurate values of the dot size (height and base) to determine the absorption peaks and corresponding absorption coefficient. Theoretical calculations are verified with the reported experimental and theoretical results.

II. THEORETICAL MODEL

In the effective mass approximation, the envelope wave function for an electron or hole is¹⁹

$$\psi(x, y, z) = \sqrt{\frac{8}{L_{bx}L_{by}L}} \sin\left(\frac{l_1\pi x}{L_{bx}}\right) \left(\frac{l_2\pi y}{L_{by}}\right) \left(\frac{l_3\pi z}{L}\right), \quad (1)$$

where L is the height of the quantum box, L_{bx} and L_{by} are the base width in the x and y directions, respectively. Integers (l_1, l_2, l_3) define the quantum numbers.

^{a)}Electronic mail: uperera@gsu.edu

The confinement energies of the carrier $E_{carrier}^{states}(l_i)$ (in units of $\frac{\hbar^2}{m_{carrier}^*W^2}$) for a finite well can be approximated as²⁰

$$E_{carrier}^{states}(l_i) = \frac{2P_{carrier}^2}{(P_{carrier} + 1)^2} \sum_i \left[\left(\frac{l_i\pi}{2} \right)^2 - \frac{1}{3(P_{carrier} + 1)^3} \left(\frac{l_i\pi}{2} \right)^4 - \frac{27P_{carrier} - 8}{180(P_{carrier} + 1)^6} \left(\frac{l_i\pi}{2} \right)^6 \right], \quad (2)$$

where the subscript ‘‘carrier’’ in the equation is for either the (e) electron, (hh) heavy holes, or (lh) light holes with respective effective masses considered for the calculations. The superscript ‘‘states’’ defined as either ‘‘initial’’ or ‘‘final’’ subband energy level of the QD.

The integer l_i , where $i = 1, 2, 3, \dots$ in Eq. (2) denotes the quantum numbers for the initial and final levels as either for (e) electrons, (hh) heavy holes, or (lh) light holes. The well strength parameter $P_{carrier}$ is defined as $P_{carrier} = (\sqrt{2m_0m_{carrier}^*}V_0/\hbar)W/2$ for (e) electrons, (hh) heavy holes, or (lh) light holes depending on the effective mass considered for the calculations. $W = L, L_{bx}$ or L_{by} is the well width in the corresponding direction and V_0 is the depth of the well (conduction/valance band). The rest mass of the electron and effective masses of carriers (electrons or holes) are $m_0, m_{carrier}^*$, respectively. The carrier effective mass will also be different for the conduction and valance bands.

The photon energy needed for an intersubband transitions in a QD is given by

$$\hbar\omega = E_{carrier}^{final}(l_i) - E_{carrier}^{initial}(l_i), \quad (3)$$

where $E_{carrier}^{final}$ and $E_{carrier}^{initial}$ are final and initial subband energy states, respectively.

The absorption coefficient is described as the reciprocal of the depth of penetration of the incident beam into a material, i.e., it is equal to the depth at which the energy of the incident beam has decreased/attenuated by the material to (e^{-1}) of its initial value at a distance from the surface.²¹ The absorption coefficient is of dimension (length^{-1}). The optical absorption coefficient of a QD with height L and base lengths L_{bx} and L_{by} is calculated as¹⁹

$$\alpha_{subband} = \frac{A_{real}}{L_{bx}L_{by}L} \sum_i g(l_i) \times \delta \left[E_{carrier}^{final}(l_i) - E_{carrier}^{initial}(l_i) - \hbar\omega \right], \quad (4)$$

where $g(l_i)$ is the degeneracy factor²² defined by the final energy level of the QD and A_{real} is a constant¹⁹ in terms of $P_{carrier}$. We define the selection rule for available transitions²² as $\Delta l = 1$. The QD ground state has the quantum numbers $(l_1, l_2, l_3) = (1, 1, 1)$; the second level (first excited state) is $(l_1, l_2, l_3) = (1, 2, 1)$ or $(2, 1, 1)$ (for $L_{bx}=L_{by}$) with a degeneracy²² of 2.

We define ratio of base to height as $\gamma_x = (\frac{L}{L_{bx}})$ and $\gamma_y = (\frac{L}{L_{by}})$; thus Eq. (4) takes the form

$$\alpha_{subband} = \frac{\gamma_x\gamma_y A_{real}}{L^3} \sum_i g(l_i) \times \delta \left[E_{carrier}^{final}(l_i) - E_{carrier}^{initial}(l_i) - \hbar\omega \right]. \quad (5)$$

The observed optical spectra from an ensemble of QDs are considered as the superposition of the contributions from each individual dot in the ensemble. Although both Gaussian and Lorentzian distribution functions are reported in the literatures,^{16,17} the experimental works^{23,24} indicate Gaussian distributions. Using a Gaussian distribution, the dot height (L) can be represented as

$$G(L) = \left(\frac{1}{S} \right) \left(\frac{1}{\sqrt{2\pi}} \right) \exp \left[-\frac{(L - L_{avg})^2}{2S^2} \right], \quad (6)$$

where L_{avg} is the average dot height of the system and S is the standard deviation. Let ξ be the relative standard deviation of the dot height given by

$$\xi = \frac{S}{L_{avg}}, \quad (7)$$

$$G(L) = \frac{1}{\xi L_0} \times \frac{1}{\sqrt{2\pi}} \exp \left[-\frac{\left(\frac{L}{L_{avg}} - 1 \right)^2}{2\xi^2} \right]. \quad (8)$$

Now following the equations in Refs. 18 and 19, we get the equation for absorption coefficient considering Gaussian distribution of the dot dimension and finite barrier approximation for intersubband transitions for QD as

$$\frac{\alpha_{subband}}{\beta_{subband}} = \frac{\gamma_x\gamma_y}{\xi} \times \frac{\pi^2\hbar^2}{m_{carrier}^*L_{avg}} \sum_i g(l_i) \times \sum_{j=1}^N \frac{\frac{1}{L_r^3} \exp \left[-\frac{\left(\frac{L}{L_{avg}} - 1 \right)^2}{2\xi^2} \right]}{\left[E_{carrier}^{final}(l_i) - E_{carrier}^{initial}(l_i) - \hbar\omega \right]_{L=L_r}}, \quad (9)$$

where N is the number of roots (L_r) of the function $E_{carrier}^{final}(l_i) - E_{carrier}^{initial}(l_i) - \hbar\omega = 0$ and $\beta_{subband}$ is a dimensionless constant defined as¹⁹

$$\beta_{subband} = \frac{A_{real}}{\sqrt{2\pi}} \times \frac{m_{carrier}^*}{\pi^2\hbar^2}.$$

III. RESULTS AND DISCUSSIONS

To begin with, we compare our results with reported theoretical results²⁵ by Feng *et al.* We compute the heavy hole transition levels for the reported $\text{In}_{0.56}\text{Ga}_{0.44}\text{N}/\text{GaN}$ QD size in Ref. 25 (i.e., $L_{avg} = 5$ nm). Considering the relative standard deviation (ξ) value as 0.02, it is observed that our computed peak transitions for the (hh2) 2nd and (hh3) 3rd (hh) heavy hole levels to (hh1) ground levels are at energies 0.027 eV and 0.051 eV, closely matched the reported values²⁵ of ~ 0.025 eV and ~ 0.052 meV, respectively.

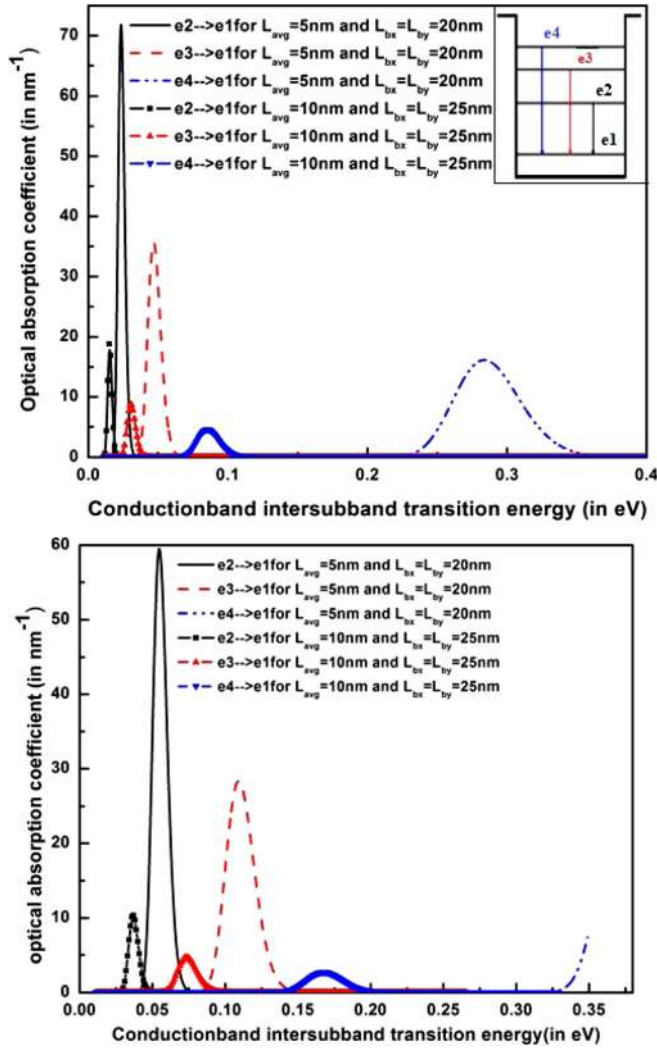


FIG. 1. Absorption spectra of the lowest three available transitions in the conduction band. Transitions are between excited states and the ground states of the InN/GaN (upper panel) and InAs/GaAs (lower panel) QDs. Curves without symbols are for $L_{avg} = 5$ nm and $L_{bx} = L_{by} = 20$ nm QD and curves with symbols are for $L_{avg} = 10$ nm and $L_{bx} = L_{by} = 25$ nm QD. Inset shows the transitions from different excited levels to the ground level.

In our calculations for InAs/GaAs and InN/GaN dots, the effective masses were calculated through a linear extrapolation between the effective masses of InAs, GaAs and InN, GaN, respectively.^{26,27} The band offset ratio $\Delta EC:\Delta EV$ for both sets was considered to be 55:45.²⁷

Figures 1 and 2 show the optical absorption coefficient corresponding to available intersubband electronic transitions in the conduction band and heavy hole transitions in the valance band, respectively. Calculations were carried out

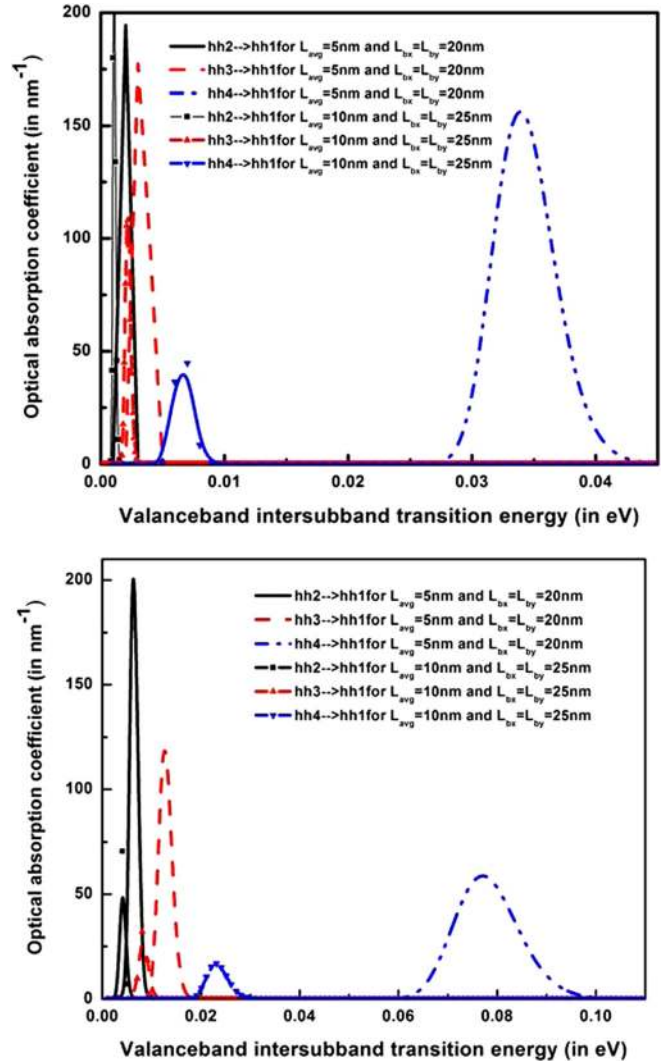


FIG. 2. Absorption spectra of the lowest three available transitions in the valance band. Transitions are between excited states and the ground states of the InN/GaN (upper panel) and InAs/GaAs (lower panel) QDs. Curves without symbols are for $L_{avg} = 5$ nm and $L_{bx} = L_{by} = 20$ nm QD and curves with symbols are for $L_{avg} = 10$ nm and $L_{bx} = L_{by} = 25$ nm QD.

for different sets of the InAs/GaAs and InN/GaN dots with different sizes ($L_{avg} = 5$ nm and 10 nm) and relative standard deviation (ζ) of 0.05. In the following figures, we show only the available transitions for (e) electronic transitions in conduction band and (hh) heavy hole transitions in valance band. In the inset of Figure 1, available intersubband transition is shown for the conduction band, similar transitions occur in the case of valance band shown in Figure 2. It is observed from Figure 1 that there is a redshift in the energy

TABLE I. Calculated intersubband transitions energy (in eV) using the present model in the conduction and valance bands for InN/GaN and InAs/GaAs QD with different sets of height and base (in nm) as shown in Figures 1 and 2.

Composition of the QD	Height (L_{avg}) of the QD (in nm)	Base ($L_{bx} = L_{by}$) of the QD (in nm)	Transitions in the conduction band (in eV)			Transitions in the valance band (in eV)		
			(e2-e1)	(e3-e1)	(e4-e1)	(hh2-hh1)	(hh3-hh1)	(hh4-hh1)
InN/GaN	5	20	0.023	0.047	0.283	0.0021	0.0030	0.0250
	10	25	0.015	0.030	0.085	0.0011	0.0022	0.0070
InAs/GaAs	5	20	0.055	0.110		0.0061	0.0131	0.0771
	10	25	0.037	0.074	0.169	0.0041	0.0081	0.0231

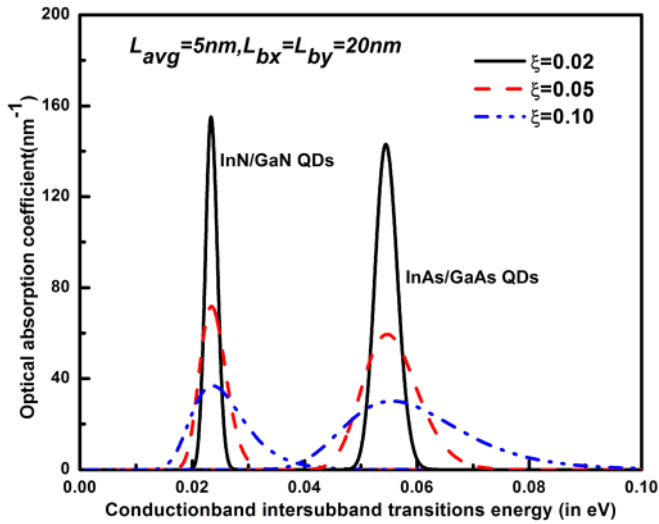


FIG. 3. Variation of absorption coefficient with electron subband transitions energy for different dot size distributions (relative standard deviation ξ) for the dot dimensions $L_{avg} = 5$ nm and $L_{bx} = L_{by} = 20$ nm.

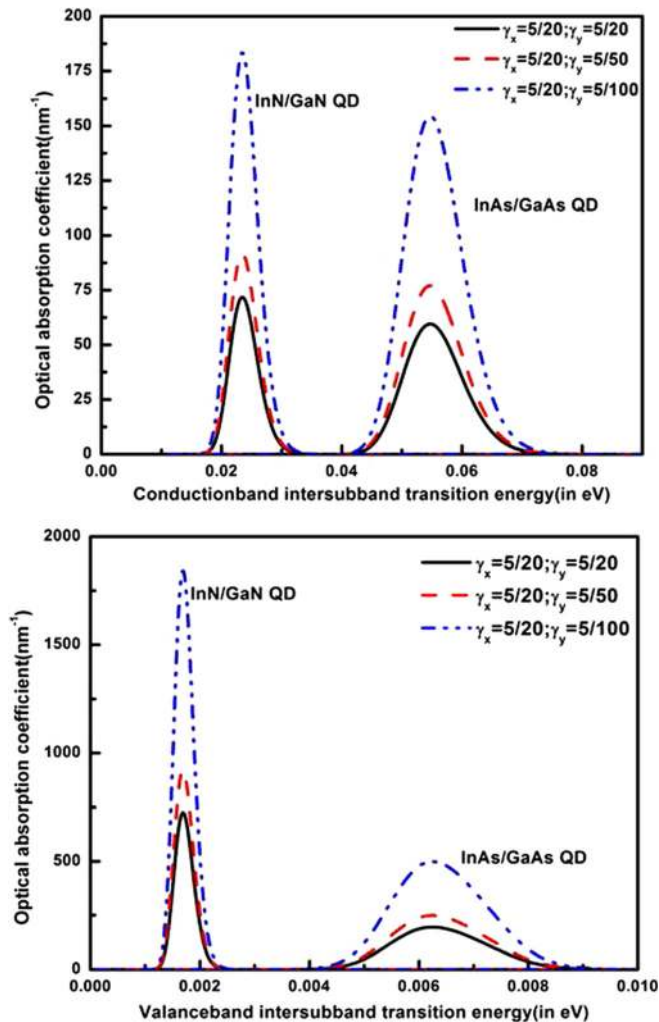


FIG. 4. Variation of absorption coefficient with electron (upper panel) and hole (lower panel) subband transitions energy for different aspect ratios (γ_x and γ_y) of InN/GaN and InAs/GaAs QDs. As the aspect ratio in the Y direction (γ_y) reduced, the absorption coefficient increases. Similar results will be expected by changing the aspect ratio in the X direction (γ_x).

and also a decrease in the absorption coefficient value with increasing dot size. It is also noted that for higher dot size, the change in the energy with changing dot size is not very significant. In Figure 1 for the InN/GaN QD, we observed the three lowest available transitions for smaller dots, whereas in case of InAs/GaAs QDs for 5 nm QD, only the transition between the first two excited states to the ground state (e_2 to e_1 and e_3 to e_1) is possible, further with a standard deviation of 0.05, all the dots in the ensemble not taking part in the transitions. Details of the peak energy corresponding to their transition energy levels are given in Table I.

Figure 3 shows the variation of the absorption coefficient for different standard deviations (ξ) from a QD samples with average dot size $L_{avg} = 5$ nm and $L_{bx} = L_{by} = 20$ nm. As seen in Figure 3, for homogeneous dot ensemble, the absorption spectra will be much narrower keeping the peak transition energy the same.

The absorption coefficient for both conduction and valance bands with different aspect ratios ($\gamma_x (= \frac{L_x}{L_{bx}})$ and $\gamma_y (= \frac{L_y}{L_{by}})$, keeping the height of the QD constant ($L_{avg} = 5$ nm) is plotted in Figure 4. As seen in Figure 4, as γ_y decreases (keeping L constant and increasing L_{by}), the absorption coefficient increases. However, this will not change the peak position.

Although in general energy levels will change with the aspect ratio (i.e., with the well width), considering only the first ($l = 1$) energy levels for 50 nm and 100 nm well widths for 1D quantum wells (QWs), the variation between 50 nm and 100 nm well width is ~ 0.002 eV, which is negligible.

There is also recent interest in quantum dash or elongated quantum dot^{28,29} structures which have longer dimensions (than the QDs) in the range of ~ 100 nm. The curve corresponding to $\gamma_x (= \frac{5}{100})$ in Figure 4 shows the absorption coefficient for such structures. For interband transitions, the absorption peak position can change with changing aspect

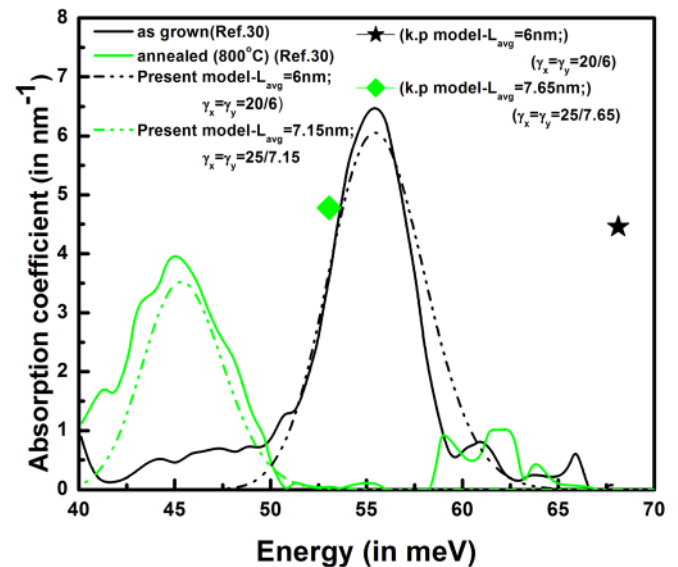


FIG. 5. Absorption spectra of as grown and annealed (at 800°C) QDs as reported in Ref. 30 shown in solid lines. Computed results of absorption coefficient values for reported QDs structures (in Ref. 30) are shown in dashed lines. Calculated results using 8 band k.p method for both as grown and annealed QDs, respectively, are shown by symbols (\star and \blacklozenge) in the same graph.

TABLE II. QD parameters, i.e., height and base (in nm) to fit the reported experimental absorption peaks³⁰ using the present model. Also, a comparison between the present model and 8 band k.p model³¹ to fit the experimental results as shown in Figure 5.

Experimental absorption peak (in meV) ³⁰	QD parameters (in nm)						
	Experimental ³⁰		8 band k.p ³¹		Present model		
	Height	Base	Height	Base	Height	Base	
As grown	56	6.00	20.0	8.50	20.0	6.00	20.0
Annealed at 800 °C	45	7.65	25.0	9.61	25.0	7.15	25.0

ratio, however in the case of intersubband transitions, the change in the peak position is negligible but can have a significant change in the absorption coefficient, as shown in Figure 4.

The accuracy of the energy levels of a QD calculated using Eq. (2) depends on the width and the depth of the well, defined by the band offset of the QW. Energy values are of high accuracy if the energy levels are confined in the bottom of the QW, i.e., if the energy levels have energy less than half of the QW depth. In our calculation, the well widths considered vary from ~ 5 nm to ~ 100 nm depending upon the reported dimensions for the QDs and Qdashes, where the height varies from ~ 5 to 20 nm and the base widths vary from ~ 20 to 100 nm. For QD, the possible levels are (1, 1, 1), (1, 2, 1), (1, 1, 2), (2, 1, 1), (1, 2, 2), (2, 1, 2), (2, 2, 2), considering only the first two energy levels of a QW, depending upon the size of the QD (height and base of the QD). The lowest electronic level, i.e., (1, 1, 1) for a QD with a height and base of 5 nm, is calculated considering a 5 nm 1D InAs/GaAs QW. This level is at 0.1576 eV, which is below the half way mark of the depth of the QW considered. Hence, for the QD with 5 nm size the lowest calculated level has high accuracy. For the 1D QW with 15 nm width and similar composition and depth, the lowest and first excited levels are at 0.0303 eV and 0.1202 eV, respectively, still below the half way mark of the QW. As the well width is increased, the levels come down and should be below the half of the well depth for same QD composition. Beyond this region, the error increases and a different approximation as suggested in Ref. 20 may be needed.

In order to further validate the model, our calculated results were compared with experimental results.³⁰ Zibik *et al.*³⁰ reported intersublevel absorption spectroscopy results for InAs/GaAs QDs. They reported an absorption peak at 56 meV for a sample with average height and width of ~ 6 and ~ 20 nm, respectively. The sample was annealed at a temperature of 800 °C, causing the height and width to

change to 7.65 nm and 25 nm, respectively, shifting the absorption peak position to 45 meV. The present model predicts absorption peak energies at 56 meV and 45 meV (for as grown QDs with a height of 6 nm and width of 20 nm, and annealed at 800 °C with a height of 7.15 nm and width 25 nm) in accordance with the reported QD experimental values, as seen by the dashed curves in Figure 5. The reported experimental absorption³⁰ value (in %) converted to absorption coefficient (in nm^{-1}) is shown in Figure 5. The full widths at half maxima of the calculated curves and absorption coefficient (in nm^{-1}) are well matched with the experimental absorption curves for dot distribution with heights of 6 nm and 7.15 nm with a relative standard deviation (ξ) value of 0.025. The width of the dot is connected to the height with the aspect ratio. Details of the experimental and calculated results for Figure 5 are shown in Table II. The reported experimental results are also computed using 8 band k.p model.³¹ A comparison between the 8 band k.p model and present model is shown in the Table II with the experimental results. The calculated results using 8 band k.p for reported as grown and annealed QD sizes, (height 6 nm and base 20 nm) and (height 7.65 nm and base 25 nm), indicate peaks at 68 meV and 53 meV, respectively, as pointed out in Figure 5; while our model gives the values at 56 meV and 38 meV, respectively, for those QD parameters. It is shown that the present model provides much better results with the experimental absorption peak energies than the 8 band k.p calculations.

In Table III, some reported experimental results^{32,33} verified with our theoretical model are shown.

Many-body properties, such as plasmonic effect in general could affect the intersublevel transitions of QDs (Refs. 34 and 35) but in the present form, the current model cannot address those concerns and need further research. However, the close agreement of our calculated results with the experimental results indicates negligible effects for the size of the dots we have considered here, as indicated elsewhere.^{34,35}

TABLE III. A comparison in the QD parameters (height and base in nm) with the experimental values to match different reported experimental peak transition energies^{32,33} calculated using the present model.

Experimental report		QD Parameters (in nm)			
		Experimental		Present model	
		Height	Base	Height	Base
Composition of the QD	Reported Peak energy (in eV)				
InAs/GaAs (Ref. 32)	0.247	5	20	5	18
InAs/GaAs (Ref. 33)	0.073	5	15	5	17

IV. CONCLUSION

In conclusion, an analytical model is reported for the calculation of the intersubband transitions energy and absorption coefficients of different QD ensembles. Our modelling considered the QDs approximated as quantum boxes with finite potential barriers and a size distribution described by a Gaussian function. The effects of size nonuniformity on the electron and hole intersubband optical absorption spectrum of a quantum dot systems were analyzed. It was shown that the optical absorption spectrum of quantum dots depends strongly on the dot size distribution. We therefore expect to exploit, in practice, the advantages of quantum dots in different applications, such as photodetectors. Experimental results on absorption spectra agree satisfactorily with the proposed model. This agreement is very difficult to achieve with the conventional modellings where QDs are approximated with infinite potential barriers. This work serves to further the understanding of self-assembled quantum dots with the goal of improving devices considering intersubband transitions.

ACKNOWLEDGMENTS

This work was supported in part by the U.S. Army Research Office under Grant No. W911NF-12-2-0035 monitored by Dr. William W. Clark, and in part by the U.S. National Science Foundation under Grant No. ECCS-1232184. Authors appreciate the helpful comments by Dr. S. Manson and his careful reading of the manuscript.

¹P. Bhattacharya and Z. Mi, *Proc. IEEE* **95**, 1723 (2007).

²T. Frost, A. Banerjee, K. Sun, S. L. Chuang, and P. Bhattacharya, *IEEE J. Quantum Electron.* **49**, 923 (2013).

³A. V. Barve, S. J. Lee, S. K. Noh, and S. Krishna, *Laser Photon. Rev.* **4**, 738 (2010).

⁴P. Martyniuk and A. Rogalski, *Prog. Quantum Electron.* **32**, 89 (2008).

⁵P. Madejczyk, W. Gawron, P. Martyniuk, A. K. Eblowski, A. Piotrowski, J. Pawluczyk, W. Pusz, A. Kowalewski, J. Piotrowski, and A. Rogalski, *Semicond. Sci. Technol.* **28**, 105017 (2013).

⁶A. M. Itsuno, J. D. Phillips, and S. Velicu, *Appl. Phys. Lett.* **100**, 161102 (2012).

⁷Y.-F. Lao, P. K. D. D. P. Pitigala, A. G. Unil Perera, E. Plis, and S. S. Krishna, *Appl. Phys. Lett.* **103**, 181110 (2013).

⁸E. A. DeCuir, Jr., G. P. Meissner, P. S. Wijewarnasuriya, N. Gautam, S. Krishna, N. K. Dhar, R. E. Welsler, and A. K. Sood, *Opt. Eng.* **51**, 124001 (2012).

⁹A. Rogalski, J. Antoszewski, and L. Faraone, *J. Appl. Phys.* **105**, 091101 (2009).

¹⁰A. Rogalski, *J. of Phys.: Conf. Series.* **146**, 012030 (2009).

¹¹G. Ariyawansa and A. G. U. Perera, in *Handbook of Self Assembled Semiconductor Nanostructures Novel Devices in Photonics and Electronics*, edited by M. Henini (Elsevier Ltd., 2007).

¹²R. Notzel, *Semicond. Sci. Technol.* **11**, 1365 (1996).

¹³P. Bhattacharya, S. Ghosh, and A. D. Stiff-Roberts, *Annu. Rev. Mater. Res.* **34**, 1 (2004).

¹⁴I. R. Grant, "Optical materials in defence systems technology," *Proc. SPIE* **5621**, 58 (2004).

¹⁵A. D. Stiff-Roberts, *J. Nanophotonics* **3**, 031607 (2009).

¹⁶W. Y. Wu, J. N. Schulman, T. Y. Hsu, and U. Efron, *Appl. Phys. Lett.* **51**, 710 (1987).

¹⁷L. Ferreira and A. J. L. Alves, *Nanotechnology* **15**, 975 (2004).

¹⁸S. Kumar and D. Biswas, *J. Appl. Phys.* **102**, 084305 (2007).

¹⁹S. Kabi, S. Panda, and D. Biswas, *J. Appl. Phys.* **109**, 053110 (2011).

²⁰D. L. Aronstein and C. R. Stroud, Jr., *Am. J. Phys.* **68**, 943 (2000).

²¹J. Singh, *Electronic and Optoelectronic Properties of Semiconductor Structures* (Cambridge University Press, 2003) p. 360.

²²S. Maimon, E. Finkman, G. Bahir, S. E. Schacham, J. M. Garcia, and P. M. Petroff, *Appl. Phys. Lett.* **73**, 2003 (1998).

²³Q. D. Zhuang, J. M. Li, Y. P. Zeng, L. Pan, H. X. Li, M. Y. Kong, and L. Y. Lin, *J. Cryst. Growth* **200**, 375 (1999).

²⁴K. Yamaguchi, K. Yujobo, and T. Kaizu, *Jpn. J. Appl. Phys. Part 2* **39**, L1245 (2000).

²⁵S.-W. Feng, *Thin Solid Films* **516**, 7695 (2008).

²⁶See <http://www.ioffe.ru/SVA/NSM/> for New Semiconductor Materials. Characteristics and Properties.

²⁷D. Biswas, S. Kumar, and T. Das, *Thin Solid Films* **515**, 4488 (2007).

²⁸A. Musiał, G. Sek, P. Podemski, M. Syperek, J. Misiewicz, A. Löffler, S. Höfling, and A. Forch, *J. Phys.: Conf. Ser.* **245**, 012054 (2010).

²⁹M. H. T. Dastjerdi, M. Djavid, S. Arafin, X. Liu, P. Bianucci, Z. Mi, and P. J. Poole, *Semicond. Sci. Technol.* **28**, 094007 (2013).

³⁰E. A. Zibik, W. H. Ng, L. R. Wilson, M. S. Skolnick, J. W. Cockburn, M. Gutierrez, M. J. Steer, and M. Hopkinson, *Appl. Phys. Lett.* **90**, 163107 (2007).

³¹H. Jiang and J. Singh, *Phys. Rev. B* **56**, 4696 (1997).

³²Y.-F. Lao, S. Wolde, A. G. Unil Perera, Y. H. Zhang, T. M. Wang, H. C. Liu, J. O. Kim, T. Schuler-Sandy, Z.-B. Tian, and S. S. Krishna, *Appl. Phys. Lett.* **103**, 241115 (2013).

³³J. Phillips, P. Bhattacharya, S. W. Kennerly, D. W. Beekman, and M. Dutta, *IEEE J. Quantum. Electron.* **35**, 936 (1999).

³⁴R. Heitz, F. Guffarth, I. Mukhametzanov, M. Grundmann, A. Madhukar, and D. Bimberg, *Phys. Rev. B* **62**, 16881 (2000).

³⁵S. Raymond, S. Fafard, P. J. Poole, A. Wojs, P. Hawrylak, S. Charbonneau, D. Leonard, R. Leon, P. M. Petroff, and J. L. Merz, *Phys. Rev. B* **54**, 11548 (1996).